

A Fuzzy Logic Based Bidirectional On-Board Charger for Electric Vehicles with Dynamic Multiphase Operation Over All Power and Voltage Level

Uppuluri Lakshmi¹ (Assistant Professor), N. Sai Sanyasi Naidu², M. Mohan Sai³, Ch. Venkat Sai⁴, N. Rahul⁵, Ch. Sandeep Kumar⁶

DEPARTMENT OF ELECTRICAL AND ELECTRONICS ENGINEERING

SANKETIKA VIDYA PARISHAD ENGINEERING COLLEGE

VISAKHAPATNAM, INDIA.

ABSTRACT

Modern electric vehicles rely heavily on advanced power electronic devices like on-board chargers (OBCs) and DC–DC converters, which must perform reliably across a wide range of operating conditions. These systems are required to handle variations in phase number, input voltage, and battery output voltage. Meeting high-efficiency and low-cost design goals adds further complexity, especially under modern automotive standards. To address these challenges, this article proposes a novel OBC architecture capable of operating efficiently across both single-phase and three-phase configurations throughout the full output power range. Crucially, this is achieved without adding extra power components or compromising performance. A key enabler in the proposed design is the integration of **fuzzy control techniques**, which allow the system to adaptively manage diverse and uncertain input conditions, ensuring optimal performance. The result is a universal-charging solution using a single, cost-effective power processor block with high power density and efficiency. This paper also presents the design and implementation of an 11-kW bidirectional prototype for an 800-V battery system compatible with a 400-V (line-to-line) mains supply.

I. OVERVIEW

Electric cars, or EVs, are essential to the electrification process and provide a substantial contribution to the decarbonization agenda. The electrical battery, which is the main part of these cars, effectively and consistently supplies the energy needed to run the electric motors and the other electronics in the vehicle. There are now two main power ports under consideration for battery powering. Initially, the fast-charging connector is intended to supply a direct power flow from the external

charger to the dc voltage of the battery. To cut the charging time to a fraction of an hour, power ranges of 50 to 350 kW are used. Second, to encourage the wider use of EVs, the car also incorporates a flexible low-power (6.6–22 kW) ac connection that enables charging from almost any grid distribution. The on-board charger (OBC), also referred to as a converter [2], [3], has two primary purposes. The first is to supply power to any distribution grid, regardless of phase configuration, such as single-, split-, or three-phase, with voltages ranging from 85 to 265V rms, while taking grid frequencies between 40 and 65 Hz into consideration. Second, for safety purposes, the OBC makes sure that the EV battery and the mains distribution are properly isolated and have their voltages adjusted. The most successful OBC implementations have been the subject of numerous technical and review studies in recent years [2, 4, 5, 6, 7]. These studies all emphasize the need for extremely adaptable converters that can function across a broad voltage/power range. Furthermore, there has been a notable surge in interest in multiphase and bidirectional systems in recent years [8], [9]. To achieve

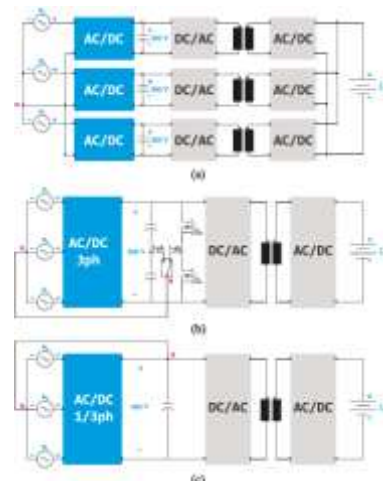


FIGURE 1. Bidirectional OBC charger architectures achieving a unity power factor consist of an ac–dc front-end and a back-end isolated dc–dc converter. (a) Phase modular ($3 \times 400\text{V}$) and (b) single (800V) front-end stage architectures that convert three-phase ac voltages u_a , u_b , u_c (or conversely, a single-phase voltage u_{abc}) to an isolated dc output voltage U_{batt} . (c) Proposed single-/three-phase single-front-end stage achieving 400V output voltage.

To meet these needs, a two-stage rectifier-based converter with power factor correction (PFC) features and a separate isolated dc–dc is typically used [10], [11]. With the help of a 400V battery and, generally, unidirectional power flow [see Fig. 1(a)], this system makes use of the well-optimized 600-V semiconductor technology [12], [13], while totem-pole rectifier-based bidirectional implementations are also feasible. However, in order to operate in a three-phase arrangement, this approach needs three power rails, which include dc–dc power converters and specialized isolating transformers. Furthermore, because of the need for numerous isolation barriers and power reference considerations, the control architecture, sensor circuits, and power supply design are complicated. When all of these design limitations are combined, performance deteriorates, power density decreases, and costs rise. A low component count and a significant decrease in isolation barriers and power references are made possible by switching from a single-phase to a three-phase rectifier [12], [14]. Furthermore, a single dc–dc converter stage can be used, which lowers control complexity and increases power density. The invention of the 1200-V SiC technology, which also makes the adoption of 800-V batteries viable, made this situation possible. This To enable OBCs that can meet contemporary vehicle-to-home, vehicle-to-vehicle, and/or vehicle-to-load charging regulations, progress has been achieved in tandem with the requirement for bidirectional power conversion [14]. Even with major advancements, state-of-the-art architectures still have a lot of limitations when it comes to operating under a variety of input and output conditions, such as 120V and 230V multiphase networks, and with varying battery charge states, such as 550V to 850V for 800V batteries. Three-phase rectifiers in particular have difficulty with single-phase setup (or split-phase operation) [15], since they need an extra current route [see Fig. 1(b)]. as well

as the application of MOSFETs or high-voltage diodes in bidirectional operation. Compared to three-phase operation, this results in a poorer power conversion efficiency and, as a result, necessitates the employment of more power electronic components. Furthermore, these boost-type three-phase rectifiers' high intermediate dc-link voltage, which is normally between 750 and 850V [16], presents further difficulties because it precludes the use of high-power-density electrolytic capacitor technology, which is typically rated only up to 450V . Consequently, a series connection is typically used, necessitating extra circuitry for voltage management and/or balancing, making the system more complicated and expensive. As a result of the large component count and the need for numerous reference levels, OBCs based on single-phase rectifiers [17], [18] provide comparable performance in single (or split)/three-phase operation at the expense of a reduced power density and efficiency levels. On the other hand, by combining power references, the use of a single three-phase based rectifier [19] allows for an improvement in power density. In contrast, single-phase operation necessitates more power electrons, which typically results in power derating and a drop in efficiency. In light of this, this article suggests a novel OBC architecture based on integrated single-phase rectifiers [1], which offers the advantages of identical single/three-phase operation with a single common-ground reference. This results in a small and economical implementation that eliminates the need for additional power devices and device stress penalties [20]. Additionally, using electrolytic capacitor technology is made easier by the 400V intermediate dc-link voltage. In single-phase operation, disconnect the grid power pulsation. The OBC is then completed by a full-bridge-based dual-active bridge (DAB) [21] to enable fully bidirectional operation, provide isolation, and adjust the intermediate dc-link voltage to the battery voltage U_{batt} . This is how the remainder of the article is structured. In Section II, the suggested OBC architecture is explained, along with how the isolated dc–dc converter and rectifier operate in three- and single-phase configurations. While Section IV examines the suggested topology to extract the primary design equations and component ratings, Section III describes the control technique to achieve adaptable functioning. The primary implementation and experimental findings are compiled in Section V, and the advantages of the suggested

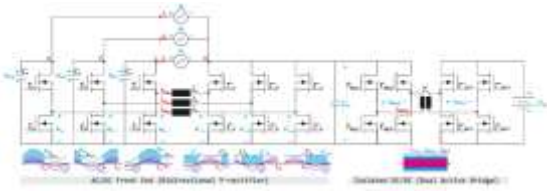


FIGURE 2. Proposed bidirectional OBC architecture in three-phase operation including the main high-frequency waveforms during a grid cycle.

converter in contrast to cutting-edge substitutes. This article is finally concluded in Section VII.

2. The Principle of Operation

A. THE SUGGESTED CONVERTER

The suggested power converter is described in length in this section. A two-stage architecture is chosen to offer a flexible solution that can adjust the battery voltage, handle large mains fluctuations, and guarantee isolation. To guarantee appropriate mains power usage, a bidirectional single-/three-phase ac-dc front-end [20] is first suggested. Second, to maintain isolation and account for fluctuations in battery voltage, an isolated DAB dc-dc converter is used. Fig. 2 displays the former along with the primary converter operational waveforms for three-phase operation.

B. AC-DC FRONT-END

This article proposes a differential rectifier based on the phase-modular buck-boost Y-rectifier concept [22]. Each of the three input stages used by this converter has a buck-boost dc-dc converter coupled to a common star "Y" point that is supplied by the positive dc-link rail. A differential rectifier with this setup experiences similar voltage and current stress in both three- and one-phase functioning. The grid neutral point *n* is linked to the positive intermediate dc-link, as explained in [20]. rail UDC. Each phase in this arrangement consists of a half-bridge leg on the dc side that is connected to the positive dc output rail (and thus also to the grid neutral point) and a half-bridge leg on the ac side that is connected to the corresponding grid terminal (which displays a positive voltage against the Y-rail). This arrangement has the benefit of enabling both single-phase and three-phase operation without the need for extra components. Relays are used for reconfiguration, which has no effect on the power range or semiconductor consumption. Grid-phase voltages *u_a*, *u_b*, and *u_c* are connected to the ac-side terminals *a*, *b*, and *c*, respectively, when three-phase operation is used [see Fig. 4(a)]. The converter then

produces sinusoidal grid currents *i_a*, *i_b*, and *i_c* in phase with the corresponding grid voltages.

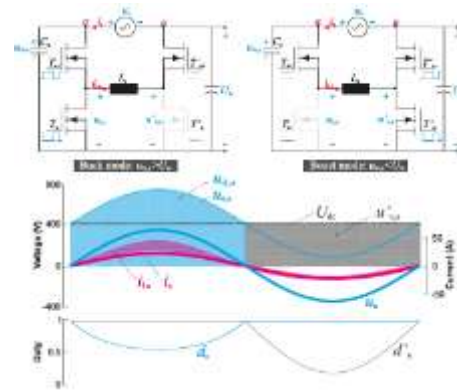


FIGURE 3. Operating modes of the ac-dc front-end module a (top), and corresponding converter waveforms (middle), and modulation parameters (bottom).

This converter operates on the same principle in every step. As shown in Fig. 3, it is discussed for phase a for simplicity's sake, and the same process is carried out for the other phases. The rail *U_{dc}* makes up the converter. Each phase in this arrangement consists of a half-bridge leg in the theater. This arrangement has the benefit of enabling both single-phase and three-phase operation without the need for extra components. Relays are used for reconfiguration; the converter supplies sinusoidal grid currents (*i_a*, *i_b*, and *i_c*) that are in phase with the corresponding grid voltages. 460 half-bridge transistors have ac and dc sides, *T_{a+}*, *T_{a-}*, and *T_{a+}*, *T_{a-}*, respectively. Within a single grid period, this design has two distinct and complementary working modes.

a) Mode I: The ac side half-bridge transistors *T_{a+}* and *T_{a-}* are complementary switched and *T_{a+}* is constantly engaged when the grid voltage is positive, *u_a* > 0. Given that the grid frequency, *f_{sw}* *f_{ac}*, is substantially lower than the converter switching frequency, the equivalent ac-side half-bridge duty cycle, *d_a*, is

$$d_a(t) = \begin{cases} \frac{U_{dc}}{U_{dc} + U_a(t)} & U_a \geq 0 \\ 1, & U_a < 0 \end{cases} \quad (1)$$

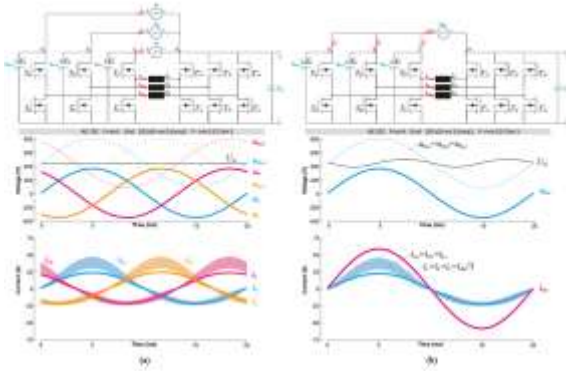


FIGURE 4. Proposed bidirectional OBC architecture including the main grid voltage and current waveforms for (a) three-phase operation and (b) single-phase operation.

where the grid-phase voltage and the intermediate dc-link voltage, $u_{dc,a} = U_{dc} + u_a$, add up to the input capacitor voltage of the ac-side half bridge. For universal grid operation with a broad grid line-to-neutral root-mean-square (RMS) voltage range of $U_{ac} = 85\text{--}265\text{VRMS}$, a strictly positive input capacitor voltage, $u_{dc,a} > 0$, is necessary to guarantee correct converter function, resulting in $U_{dc} = 400\text{--}450\text{V}$. This means that, regardless of whether the system is operating in single- or three-phase mode, 600-V rated power devices can be used for the dc-side half-bridge legs whereas 1200V SiC MOSFETs are needed for the ac-side half-bridge legs ($U_{dc,a,max} = U_{dc} + U_{a,pk} = 520\text{--}825\text{V}$).

b) Mode II: On the other hand, the converter functions in a second mode by switching the dc-side half-bridge MOSFETs T_{a+} , T_{a-} , with the higher transistor of the ac-side half-bridge T_{a+} continually engaged when the grid voltage is negative, $u_a < 0$. The resulting dc-side half-bridge duty cycle, d_a , in this instance is

$$d_a(t) = \begin{cases} 1, & U_a \geq 0 \\ \frac{U_{dc}}{U_{dc} + U_a(t)}, & U_a > 0 \end{cases} \quad (2)$$

The applied duty cycles that produce a mutually exclusive high-frequency switching activity are displayed in Fig. 3. Just three of the six half-bridges are switched simultaneously across the entire ac–dc front-end due to the ac- and dc-stages. As a result, switching losses are considerably decreased. The suggested converter, in contrast to the phase modular buck-boost Y-rectifier [22], advantageously connects the intermediate dc-link bus, U_{dc} , with the grid neutral point n . This suggests that in the event of a single-phase

connection [see Fig. 4(b)], the parallel-connected ac-side terminals a , b , and c are connected to the grid voltage u_{abc} in order to distribute the current evenly among the phase modules. The single-phase grid current i_{abc} has a return path thanks to the previously indicated connection between the grid neutral point and the positive intermediate dc-link. One of the primary benefits of the suggested converter over earlier models is that it enables full output power range operating in both single-phase and three-phase operation without requiring extra components or oversizing power devices.

Additionally, the control architecture and isolation considerations are made simpler by the fact that the ac- and dc-side half-bridge legs are referenced to the same point.

C. DC-DC Converter DAB

The back-end dc-dc converter of the suggested OBC power converter is made up of a single DAB dc-dc converter that

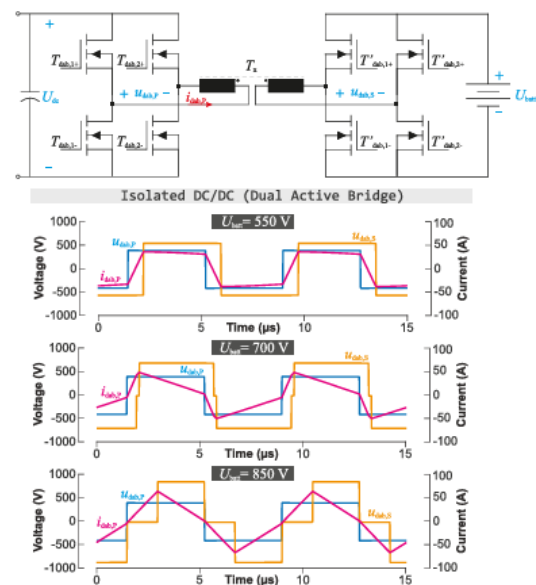


FIGURE 5. Operating modes of the dc–dc back-end module a (top), and corresponding converter waveforms (bottom).

also offers isolation by means of a high-frequency transformer. With a modulation approach that permits bidirectional power transfer and also adjusts the operating conditions to the battery voltage, this converter is made up of a primary-side full-bridge and a secondary-side full-bridge. Consequently, the suggested converter employs a single dc–dc converter to accomplish the

necessary isolated power conversion, lowering the number of necessary power devices and magnetic components and thereby further simplifying the isolation and control architecture in comparison to the state-of-the-art modular approach [see Fig. 1(a)]. Lastly, $n = 1.34$ has been determined to be the ideal turns ratio for the transformer in order to support the 400V intermediate dc-link voltage to a broad range of operational voltages typical of 800-V batteries, i.e., $U_{\text{batt}} = 550\text{--}850\text{V}$. For the most current-demanding working conditions, such as when the battery is entirely depleted, the pseudo trapezoidal control mode is employed in the low battery voltage region to minimize conduction power losses. Additionally, complete-ZVS soft-switching functioning is guaranteed in full bridges with primary and secondary sides. Furthermore, secondary duty cycle modulation is used to attain an ideal modulation profile and reduce power loss in the medium-to-high battery voltage range, as detailed in [23]. Fig. 5 shows the profiles of all these modulations.

III. STRATEGY FOR CONTROL

perform efficiently under a variety of circumstances, guaranteeing a smooth battery and sinusoidal input current consumption. Three control loops have been implemented as of right now. By sustaining a steady battery current, either positive or negative, fed by a scaled mains-voltage current level and, as a result, in phase with the mains voltage, these loops guarantee the converter operates as intended (see Fig. 6). The digital control platform is an AMD/Xilinx field programmable gate array (FPGA), which guarantees precise pulsewidth modulation generation and accurate control loop execution. First, "Control Loop A" uses the dc-link capacitor voltage stabilization to balance the power consumption of the mains and the battery. Twice every mains cycle, the dc-link voltage, U_{dc} , is measured and its peak value, $U_{\text{dc,peak}}$, is computed. To supply input to a proportional-integral (PI) controller, this value is then contrasted with the intended dc-link voltage, or 400V. To achieve the necessary mains rms current level,

$I_{\text{ac,rms}}$ to balance power consumption, the PI controller is operated at both the positive and negative zero crossings of the mains waveform. "Control Loop B" makes sure that the appropriate instantaneous mains current consumption is in phase with the mains voltage. At the conclusion of the switching time, three identical modules of this loop—each representing a mains phase—run in parallel. The output from the "MATH" unit, which basically calculates (1) and (2), plus the contribution from a PI controller add up to the required duty cycles for the rectifier's equivalent buck boost stages. The proper instantaneous mains current level is guaranteed by this team effort. "Control Loop C," the third control loop, is essential for sustaining the necessary battery current level, I_{bat} , OBJ.

To account for changes in the dc-link voltage and ensure that the battery receives the intended constant current, a PI controller is used once during each switching period. The "DAB LUT" lookup table is used to identify the best modulation scheme. The choice of this approach depends on inputs such the battery voltage, dc-link voltage, and the necessary gain, K_{DAB} .

IV. Fuzzy Logic Controller (FLC)

Fuzzy Logic Controller (FLC) is an advanced control strategy that mimics human reasoning to handle uncertain and imprecise data, making it highly suitable for complex and nonlinear systems where traditional control methods struggle. Unlike classical binary logic, which operates strictly on true or false values (1 or 0), fuzzy logic introduces a degree of flexibility by allowing values between 0 and 1, representing partial truths. This capability enables FLCs to process linguistic variables like "high," "medium," or "low," making them ideal for real-world applications where precision is difficult to define. The working of a fuzzy logic controller consists of four primary stages: fuzzification, rule base, inference engine, and defuzzification. The first stage, fuzzification, involves converting crisp numerical inputs into fuzzy values using membership functions, which define how each input belongs to different fuzzy sets.

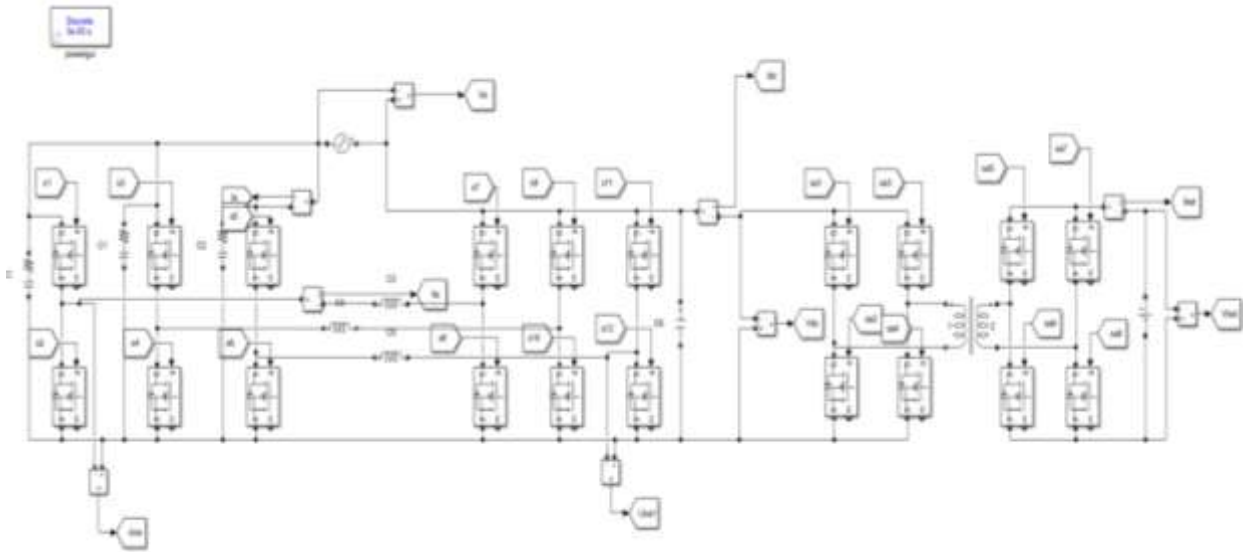
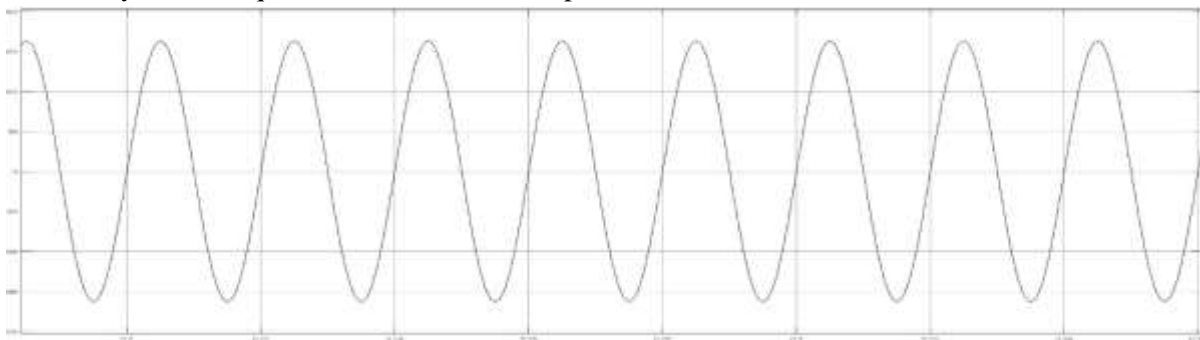


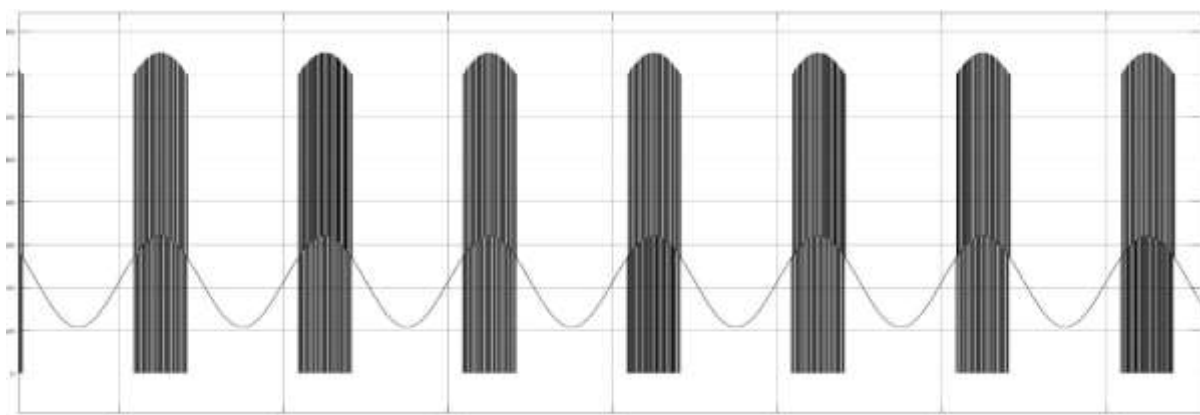
Fig 6: Single buck–boost cell operation for $U_{ac} = 230$ circuit diagram of Bidirectional of ev on boarding charging

These membership functions can take various forms, such as triangular, trapezoidal, or Gaussian, depending on the system's requirements. Once the inputs are

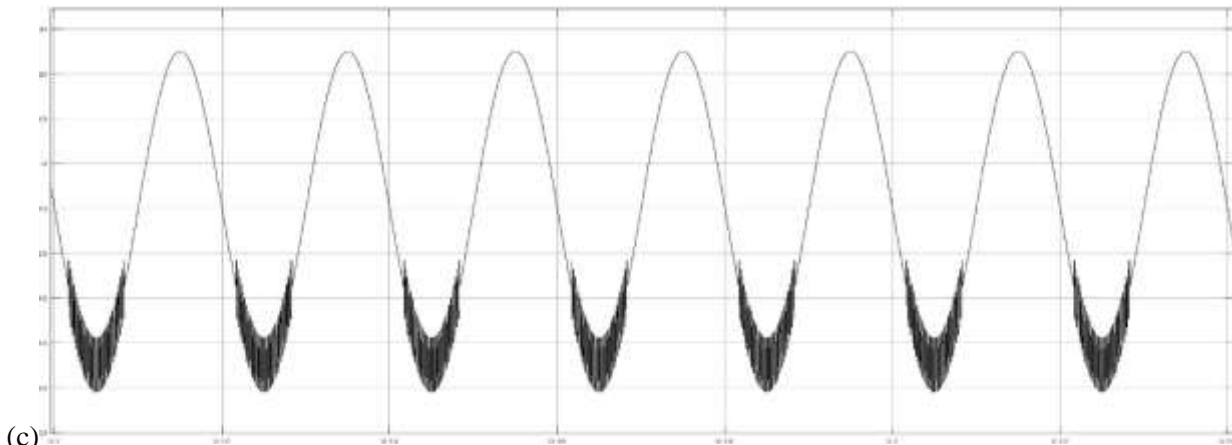
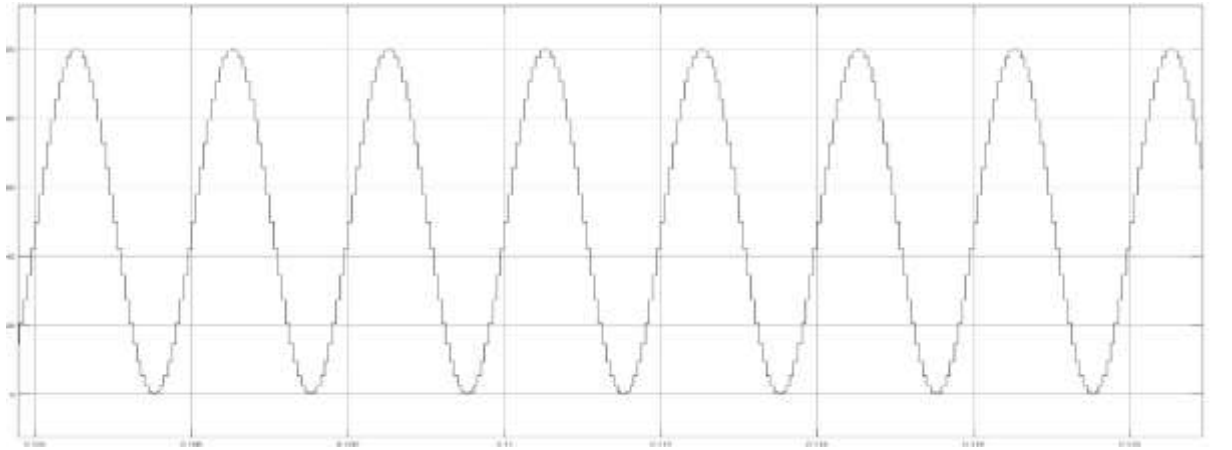
fuzzified, the rule base comes into play, consisting of a set of IF-THEN rules that define the system's behaviour.



(a)



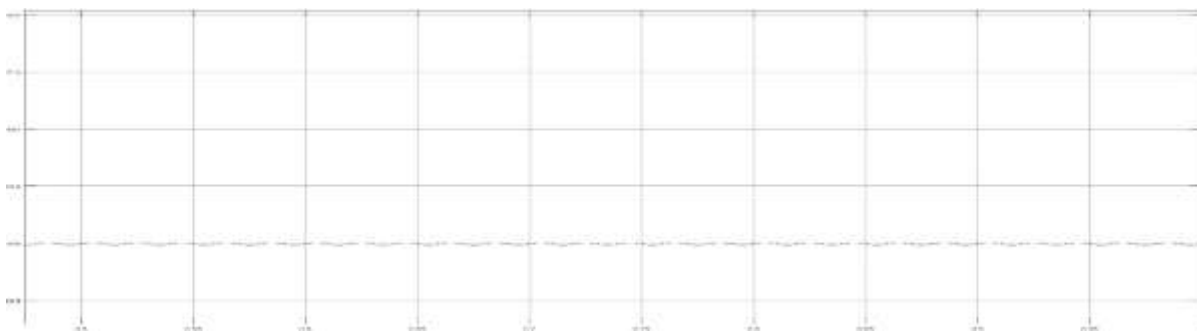
(b)



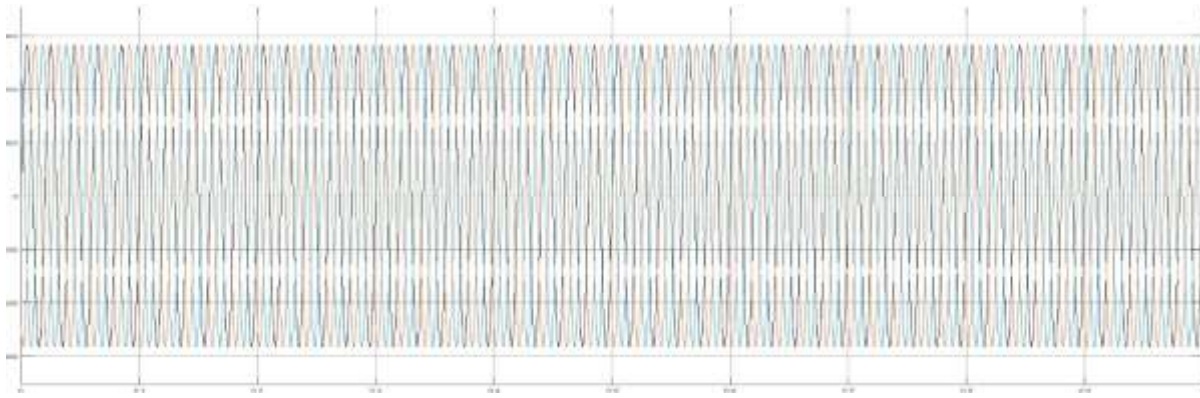
(c)

(d)

Fig 7: Single buck–boost cell operation for $U_{ac} = 230$ VRMS operating with 16 A input phase current at 100 kHz. From top to bottom: ac- and dc-side half-bridge switchnode voltage (200 V/div), grid voltage (200 V/div), grid current (50 A/div) and inductor current (50 A/div).



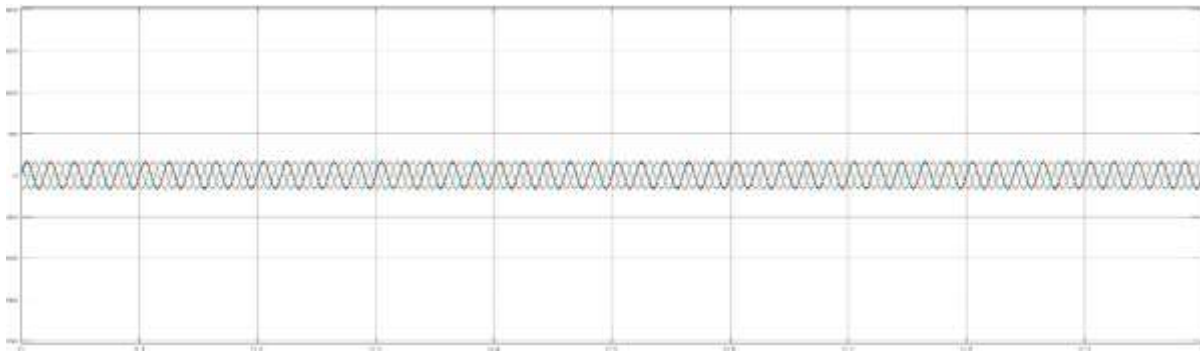
(a)



(b)



(c)



(d)

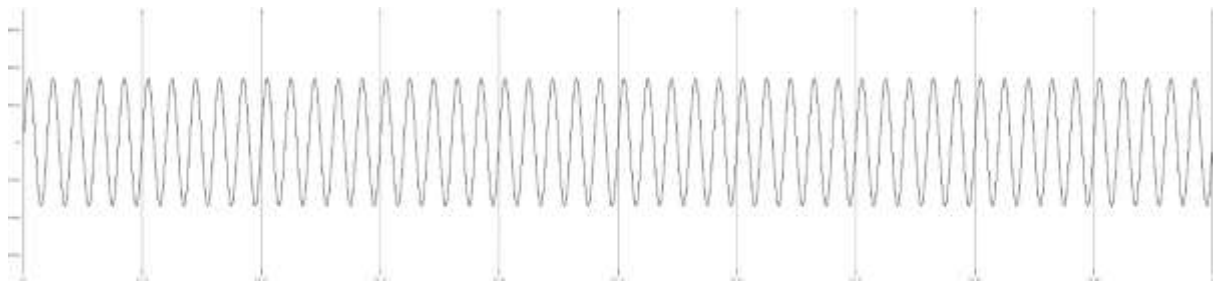
Fig 8: Three-phase operation for 400 VLL,rms, 11 kW.

These rules are formulated based on expert knowledge or empirical data and follow linguistic logic, such as "IF temperature is high, THEN reduce power." The inference

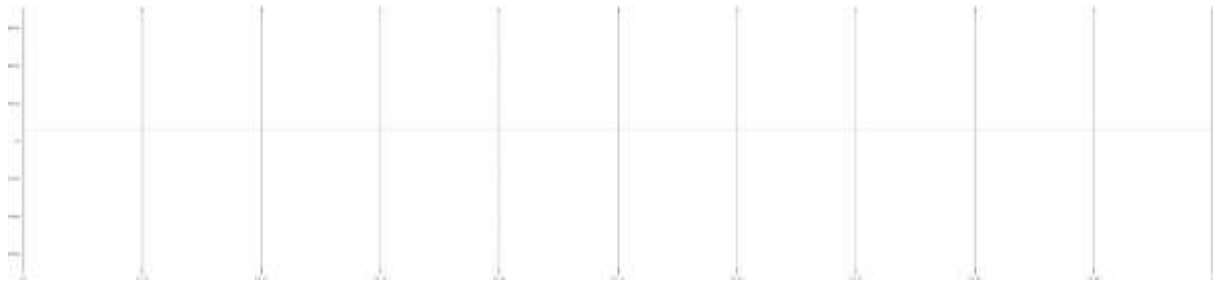
engine then processes these rules using logical operations like MIN-MAX or product inference methods to derive fuzzy outputs.



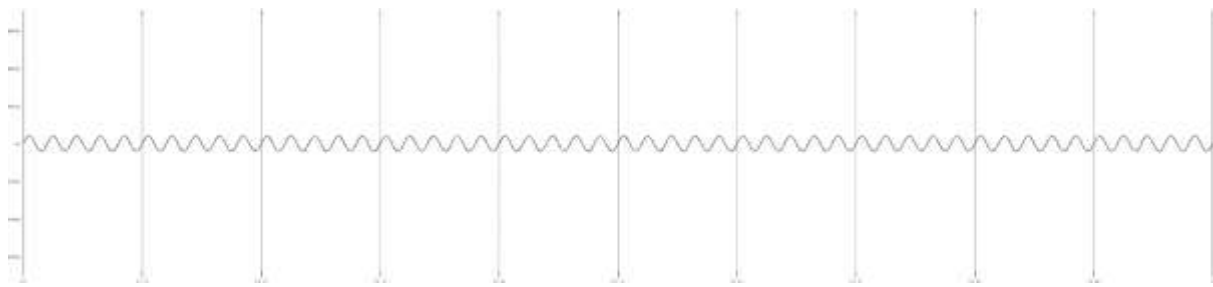
(a)



(b)



(c)



(b)

Fig 9 : Single-phase operation for 240 Vrms, 11 kW.

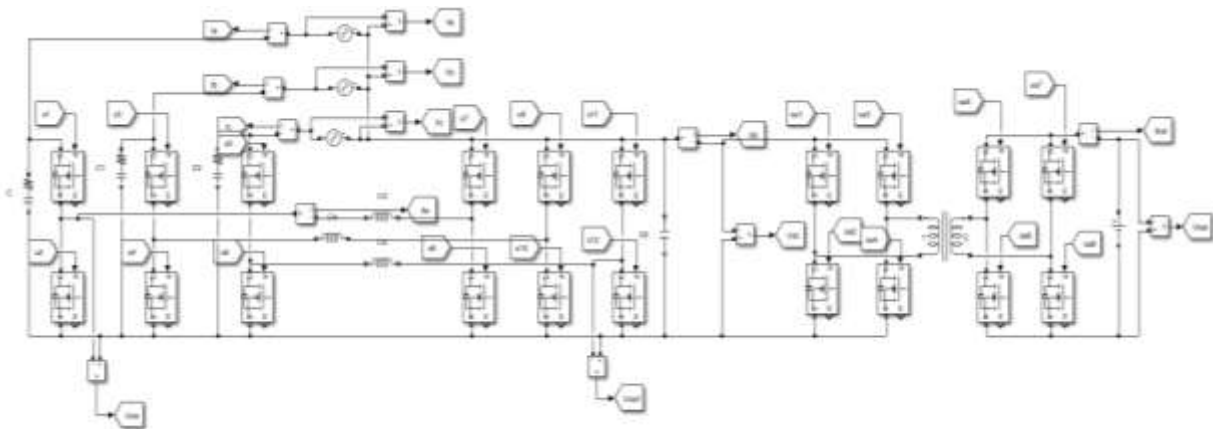


Fig 10: Three-phase operation for 400 VLL,rms, 11 kW circuit diagram of Bidirectional of ev on boarding charging

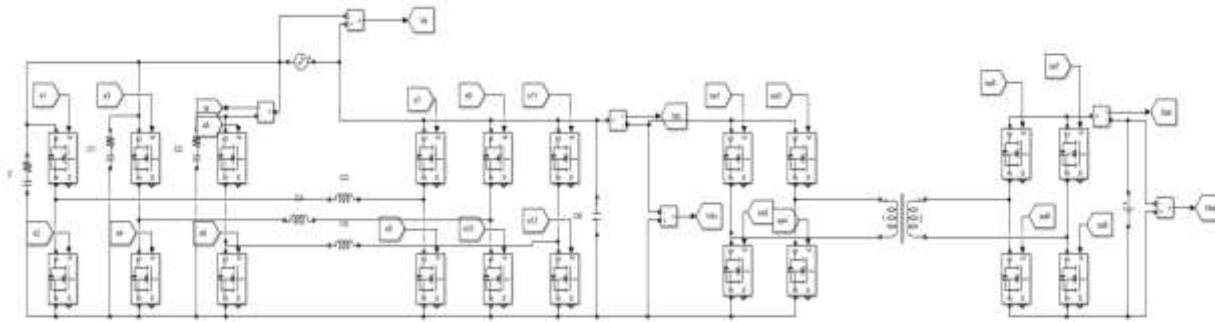


Fig 11: Single-phase operation for 240 Vrms, 11 kW circuit diagram of Bidirectional of ev on boarding charging

The final stage, defuzzification, converts the fuzzy outputs back into precise control signals, typically using methods like centroid, weighted average, or maximum membership. The FLC's ability to work with imprecise inputs and model human-like decision-making makes it highly applicable in various fields, including industrial automation, robotics, medical diagnosis, and consumer electronics. For example, in an air conditioning system, a fuzzy controller can adjust cooling levels smoothly based on room temperature and humidity instead of abrupt on-off switching, resulting in better comfort and energy efficiency. In the automotive industry, fuzzy logic is used in anti-lock braking systems (ABS) and automatic transmissions to ensure smooth gear shifting and optimal braking force. Another key application is in renewable energy systems, where FLCs optimize power output from solar panels and wind turbines by adjusting parameters dynamically based on environmental conditions. Compared to traditional PID controllers, which require precise mathematical models and struggle with system uncertainties, fuzzy logic controllers excel in handling nonlinear dynamics and disturbances. However, FLCs also have limitations, such as dependency on expert knowledge for rule formulation and challenges in tuning membership functions for highly complex systems. To address these issues, hybrid approaches integrating fuzzy logic with artificial intelligence techniques like neural networks and genetic algorithms have been developed, leading to self-adaptive and intelligent fuzzy controllers. With the rise of edge computing and the Internet of Things (IoT), FLCs are being increasingly deployed in embedded systems,

enabling real-time intelligent decision-making in smart devices. Research is ongoing to enhance fuzzy logic systems with deep learning and reinforcement learning for advanced applications like autonomous vehicles and intelligent traffic control. The future of fuzzy logic controllers lies in their synergy with modern AI and computational intelligence techniques, driving innovation in automation and smart systems. Despite evolving technologies, fuzzy logic remains a powerful and intuitive approach for handling uncertainty, making it a valuable tool for engineers and researchers in developing robust and adaptive control solutions.

VI. CONCLUSION

In order to function efficiently under diverse operating conditions while ensuring compact and cost-effective implementations, modern Electric Vehicles (EVs) increasingly rely on highly efficient and intelligent On-Board Chargers (OBCs). As EV technology progresses toward higher voltage battery systems and advanced power flow regulation, new challenges emerge, including the need for seamless single- and three-phase power operation, bidirectional energy flow, and enhanced adaptability to varying grid conditions. To address these challenges, this article introduces a novel fuzzy logic-based power conversion architecture for OBCs, integrating a Dual Active Bridge (DAB) DC-DC converter with a boost-type single-/three-phase front-end converter based on the buck-boost Y-rectifier. Unlike conventional architectures, the proposed Fuzzy Logic

Controller (FLC) enhances adaptability by dynamically adjusting power conversion parameters in response to uncertain or fluctuating grid and battery conditions. By leveraging fuzzy logic, the system intelligently determines optimal control strategies based on linguistic rules and membership functions, ensuring smooth transitions between single-phase and three-phase operations without requiring additional components or oversized power devices. Moreover, the integration of fuzzy logic enables real-time adaptive control, improving efficiency, stability, and response time under varying loads and input voltages. The simplified control structure also enhances cost-effectiveness, reducing the need for complex mathematical modeling and extensive tuning, which are inherent in traditional PID-based approaches. To validate the effectiveness of the proposed fuzzy logic-based OBC, an 11-kW bidirectional charging system was tested under a range of operating conditions, demonstrating its ability to maintain efficient and stable performance across the entire output power range. The intelligent fuzzy-based control approach not only improves power conversion efficiency and enhances grid compatibility but also supports bidirectional energy exchange for vehicle-to-grid (V2G) applications, making it a future-ready solution for next-generation EV charging infrastructures.

REFERENCES

- [1] H. Sarnago, O. Lucia, D. Menzi, and J. Kolar, "Single-/three-phase bidirectional EV on-board charger featuring full power/voltage range and a cost-effective implementation," in Proc. IEEE 17th Int. Conf. Compat., Power Electron. Power Eng., 2023, pp. 1–6.
- [2] M. Yilmaz and P. T. Krein, "Review of battery charger topologies, charging power levels, and infrastructure for plug-in electric and hybrid vehicles," IEEE Trans. Power Electron., vol. 28, no. 5, pp. 2151–2169, May 2013.
- [3] H. Sarnago and O. Lucia, "Optimized EV on-board charging power converter using hybrid DCX-DAB topology," in Proc. IEEE Appl. Power Electron. Conf. Expo., 2024, pp. 1305–1309.
- [4] H. Wouters and W. Martinez, "Bidirectional onboard chargers for electric vehicles: State-of-the-art and future trends," IEEE Trans. Power Electron., vol. 39, no. 1, pp. 693–716, Jan. 2024.
- [5] M.Y. Metwly, M. S. Abdel-Majeed, A. S. Abdel-Khalik, R. A. Hamdy, M. S. Hamad, and S. Ahmed, "A review of integrated on-board EV battery chargers: Advanced topologies, recent developments and optimal selection of FSCW slot/pole combination," IEEE Access, vol. 8, pp. 85216–85242, 2020.
- [6] S. Haghbin, S. Lundmark, M. Alakula, and O. Carlson, "Grid-connected integrated battery chargers in vehicle applications: Review and new solution," IEEE Trans. Ind. Electron., vol. 60, no. 2, pp. 459–473, Feb. 2013.
- [7] A. Khaligh and M. D'Antonio, "Global trends in high-power on-board chargers for electric vehicles," IEEE Trans. Veh. Technol., vol. 68, no. 4, pp. 3306–3324, Apr. 2019.
- [8] J. Yuan, L. Dorn-Gomba, A. D. Callegaro, J. Reimers, and A. Emadi, "A review of bidirectional on-board chargers for electric vehicles," IEEE Access, vol. 9, pp. 51501–51518, 2021.
- [9] R. P. Upputuri and B. Subudhi, "A comprehensive review and performance evaluation of bidirectional charger topologies for V2G/G2V operations in EV applications," IEEE Trans. Transp. Electrification, vol. 10, no. 1, pp. 583–595, Mar. 2024.
- [10] H. Sarnago, O. Lucia, R. Jiménez, and P. Gaona, "High power density OBC featuring power pulsating buffer," in Proc. Int. Conf. Electric Electron. Hybrid Electric Veh. Elect. Energy Manage., 2021.
- [11] H. Sarnago and O. Lucia, "Bidirectional 400-12 V dc-dc converter with improved dynamics and integrated transformer for EV applications," in Proc. IEEE Appl. Power Electron. Conf. Expo., 2024, pp. 3081–3085.
- [12] H. Sarnago, O. Lucia, R. Jiménez, and P. Gaona, "Differential-power processing on-board-charger for 400/800-V battery architectures using 650-V super junction MOSFETs," in Proc. IEEE Appl. Power Electron. Conf., 2021, pp. 564–568.
- [13] B. Whitaker et al., "A high-density, high-efficiency, isolated on-board vehicle battery charger utilizing silicon carbide power devices," IEEE Trans. Power Electron., vol. 29, no. 5, pp. 2606–2617, May 2014.
- [14] B. Li, Q. Li, F. C. Lee, Z. Liu, and Y. Yang, "A high-efficiency high density wide-bandgap device-based bidirectional on-board charger," IEEE Trans. Emerg.

Sel. Topics Power Electron., vol. 6, no. 3, pp. 1627–1636, Sep. 2018. [Online]. Available: <https://ieeexplore.ieee.org/document/8377992/>

[15] P. Papamanolis, D. Bortis, F. Krismer, D. Menzi, and J. W. Kolar, “New EV battery charger PFC rectifier front-end allowing full power delivery in 3-phase and 1-phase operation,” *Electronics*, vol. 10, no. 17, 2021, Art. no. 2069.

[16] Y. Li, J. Schäfer, D. Bortis, J. W. Kolar, and G. Deboy, “Optimal synergetic control of a three-phase two-stage ultra-wide output voltage range EV battery charger employing a novel hybrid quantum series resonant DC/DC converter,” in *Proc. IEEE Workshop Control Model. Power Electron.*, 2020, pp. 1–11.

[17] T. Instruments, “GAN-based, 6,6-kw, bidirectional, onboard charger reference design,” Texas Instruments, Rep. TI PMP22650, 2021.

[18] J. Lu et al., “A modular-designed three-phase high-efficiency high power-density EV battery charger using dual/triple-phase-shift control,” *IEEE Trans. Power Electron.*, vol. 33, no. 9, pp. 8091–8100, Sep. 2018.

[19] P. Papamanolis, D. Bortis, F. Krismer, D. Menzi, and J. W. Kolar, “New EV battery charger PFC rectifier front-end allowing full power delivery in 3-phase and 1-phase operation,” *Electronics*, vol. 10, no. 17, 2021, Art. no. 2069. [Online]. Available: <https://www.mdpi.com/2079-9292/10/17/2069> [20] H. Sarnago, O. Lucia, S. Chhawchharia, D. Menzi, and J. W. Kolar, “Novel bidirectional universal 1-phase/3-phase-input unity power factor differential AC/DC converter,” *Electron. Lett.*, vol. 59, no. 13, 2023, Art. no. e12857. [Online]. Available: <https://onlinelibrary.wiley.com/doi/pdf/10.1049/el12.12857>

[21] F. Krismer and J. W. Kolar, “Efficiency-optimized high-current dual active bridge converter for automotive applications,” *IEEE Trans. Ind. Electron.*, vol. 59, no. 7, pp. 2745–2760, Jul. 2012.

[22] M. Antivachis, D. Bortis, L. Schrittwieser, and J. W. Kolar, “Three phase buck-boost Y-inverter with wide DC input voltage range,” in *Proc. IEEE Appl. Power Electron. Conf. Expo.*, 2018, pp. 1492–1499.

[23] F. Krismer and J. W. Kolar, “Closed form solution for minimum conduction loss modulation of DAB converters,” *IEEE Trans. Power Electron.*, vol. 27, no. 1, pp. 174–188, Jan. 2012.

[24] A. Darwish, A. M. Massoud, D. Holliday, S. Ahmed, and B. W. Williams, “Single-stage three-phase differential-mode buck-boost inverters with continuous input current for PV applications,” *IEEE Trans. Power Electron.*, vol. 31, no. 12, pp. 8218–8236, Dec. 2016.

[25] D. Menzi, M. Zhang, J. W. Kolar, and J. Everts, “3- ϕ bidirectional buck boost sinusoidal input current three-level SiC Y-rectifier,” in *Proc. IEEE Appl. Power Electron. Conf. Expo.*, 2021, pp. 590–598.

[26] A. Mohamed, H. Shareef, A. Mohamed, and M. A. Hannan, “**Fuzzy logic based charging algorithm for electric vehicles,**” *International Journal of Energy Research*, vol. 36, no. 6, pp. 630–643, 2012. DOI: 10.1002/er.1959

[27] S. Jain, N. S. Beniwal, and V. V. Tyagi, “**Fuzzy logic controller for a bidirectional DC-DC converter in electric vehicle applications,**” *IEEE Int. Conf. on Power Electronics, Drives and Energy Systems (PEDES)*, 2014, pp. 1–6. DOI: 10.1109/PEDES.2014.7042082

[28] H. Mahmoudi, A. K. Adnan, and M. N. Aman, “**Fuzzy logic based energy management system for hybrid electric vehicles,**” *Energy Reports*, vol. 6, pp. 1268–1279, 2020.